Structures and Properties of Injection Moldings of Crystallization Nucleator-Added Polypropylenes. II. Distribution of Higher-Order Structures

MITSUYOSHI FUJIYAMA and TETSUO WAKINO

Polymer Development Laboratory, Tokuyama Soda Co., Ltd., Tokuyama-shi, Yamaguchi-ken 745, Japan

SYNOPSIS

Flexural test specimens were injection-molded from polypropylenes added with 0.5 wt % calcium carbonate, talc, *p-tert*-dibutyl-benzoic acid monohydroxy aluminum, or *p*-dimethyl-benzylidene sorbitol under cylinder temperatures of 200–320°C. Distributions in the flow direction of higher-order structures such as a^*-axis-oriented component fraction $[A^*]$ and crystalline orientation functions and distributions in the thickness direction of higher-order structures such as crystallinity, β-crystal content, the degree of b-axis orientation to the thickness direction, $[A^*]$, and crystalline orientation functions were studied. These higher-order structures are inhomogeneous in the flow and thickness directions, which strongly influences the product properties such as mechanical and thermal properties.

INTRODUCTION

In injection molding of thermoplastics, since molten resin solidifies under inhomogeneous stress and cooling conditions, the inner structures of the molded article are inhomogeneous, influencing the product properties. Consequently, it is important in injection molding technology of thermoplastics to clarify the influences of the primary structures of resin and molding conditions on the inhomogeneous structure of the molded article.

Many studies have so far been carried out on the distribution of higher-order structures in injection-molded polypropylenes.[1-29] The shapes of moldings studied are mainly simple shape test specimens. The influences of resin characteristics such as molecular weight, molecular weight distribution, glass fiber content, talc and calcium carbonate contents, and molding conditions such as cavity thickness, cylinder temperature (resin temperature), mold temperature, injection speed, injection pressure, holding pressure, and cooling time are studied. Higher-order structures studied are crystalline texture (morphology), crystallinity, β-crystal content, crystal orientation state, degrees of crystalline and amorphous orientations, thickness of skin layer, glass fiber concentration, and orientation of talc. Directions studied are flow direction (MD) and thickness direction (ND).

In the present paper, we will report studies on the influences of kind of crystallization nucleators and cylinder temperature on distributions in the flow direction of higher-order structures such as a^*-axis-oriented component fraction $[A^*]$ and crystalline orientation functions and distributions in the thickness direction of higher-order structures such as crystallinity, β-crystal content, the degree of b-axis orientation to the thickness direction, $[A^*]$, and crystalline orientation functions in injection moldings of crystallization nucleator-added polypropylenes.

EXPERIMENTAL

Samples and Injection Molding

Samples and injection molding method have been described in the previous paper.[30]

Journal of Applied Polymer Science, Vol. 42, 2749–2760 (1991)
 CCC 0021-8995/91/102749-12$04.00

Structural Analyses

Since the lengths of the specimens were about 12.7 cm, the a^*-axis-oriented component fraction $[A^*]$ and crystalline orientation functions at the parts 2.1, 4.2, 6.3, 8.4, and 10.5 cm from the gate were measured by the methods described in the previous paper.[30]

Thin sections about 0.3 mm thick were sliced successively from the surface to the center parallel to the surface at the central parts of specimens with a microtome. $[A^*]$ and orientation functions were measured by the methods described in the previous paper.[30] Wide-angle X-ray diffractograms were measured on the sections using a rotating specimen table. Crystallinities X_c were calculated according to the Weidinger and Hermans' method.[31] β-crystal contents, K values, were obtained according to the Turner-Jones et al. method.[32] The ratios of the (040) plane reflection intensities $I(040)$ to the (110) plane reflection intensities $I(110)$, $I(040)/I(110)$, were obtained in order to study the degree of b-axis orientation to the thickness direction.[27]

RESULTS

Distribution of Higher-Order Structures in Flow Direction

Figures 1(a)–(e) show the distributions in the flow direction of the a^*-axis-oriented component fractions $[A^*]$ of specimens molded from PP, CC, TC, BA, and GA, respectively, at various cylinder temperatures. As for the PP and CC specimens, $[A^*]$ increases with increasing cylinder temperature and slightly increases on going away from the gate. As for the TC specimen, although the dependence of $[A^*]$ on cylinder temperature is weak, its change in the flow direction is large. As for the BA specimen, both the dependence on cylinder temperature and change in the flow direction of $[A^*]$ are small. As for the GA specimen, both the dependence on cylinder temperature and change in the flow direction of $[A^*]$ are very small and its $[A^*]$ is uniform.

Figures 2(a)–(d) show comparisons of the distribution of $[A^*]$ in the flow direction among samples. Although the difference of $[A^*]$ among samples is small at low cylinder temperatures, the difference increases with increasing cylinder temperature and the order of $[A^*]$ becomes PP $\approx$ CC > BA > TC $\approx$ GA. The degree of change of $[A^*]$ in the flow direction is in the order of TC > PP $\approx$ CC $\approx$ BA > GA.

Figure 3 exemplifies the distributions in the flow direction of crystalline orientation functions of each sample molded at a cylinder temperature of 240°C. The absolute values of the c-axis orientation function f_c and b-axis orientation function f_b decrease on going away from the gate for all samples. Although the a^*-axis orientation function f_{a^*} increases on going away from the gate for the TC and BA spec-

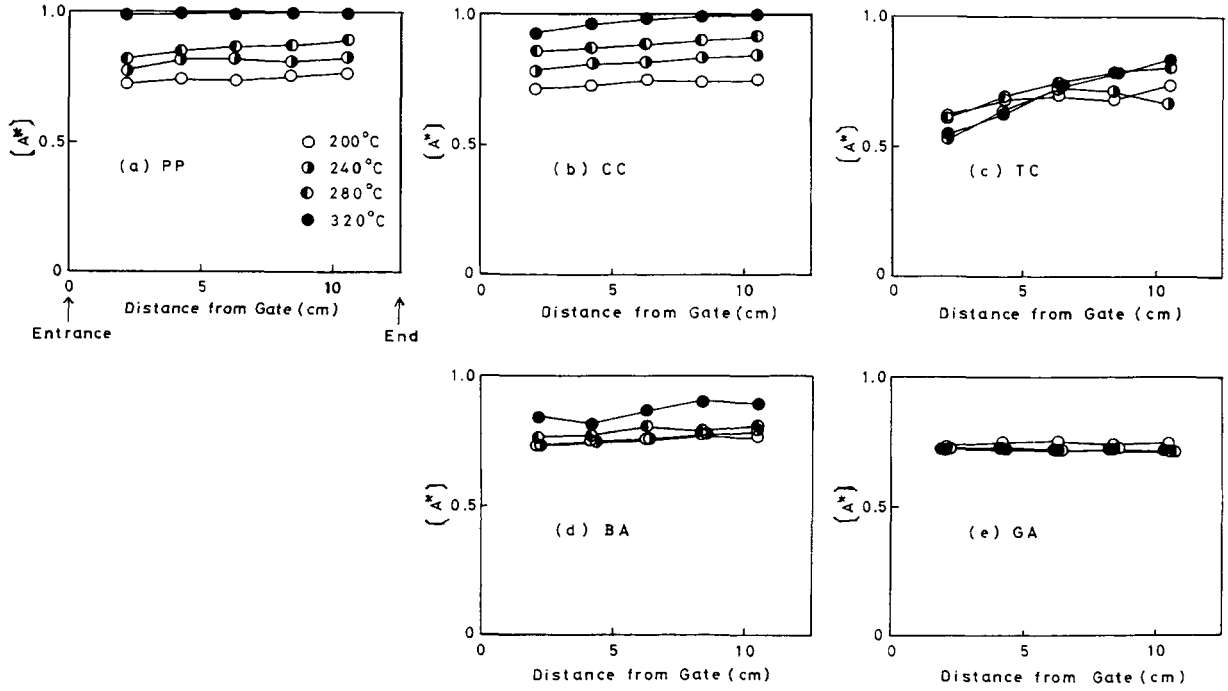

Figure 1 Distributions of a^*-axis-oriented component fraction $[A^*]$ in flow direction. Influence of cylinder temperature: (a) PP; (b) CC; (c) TC; (d) BA; (e) GA.

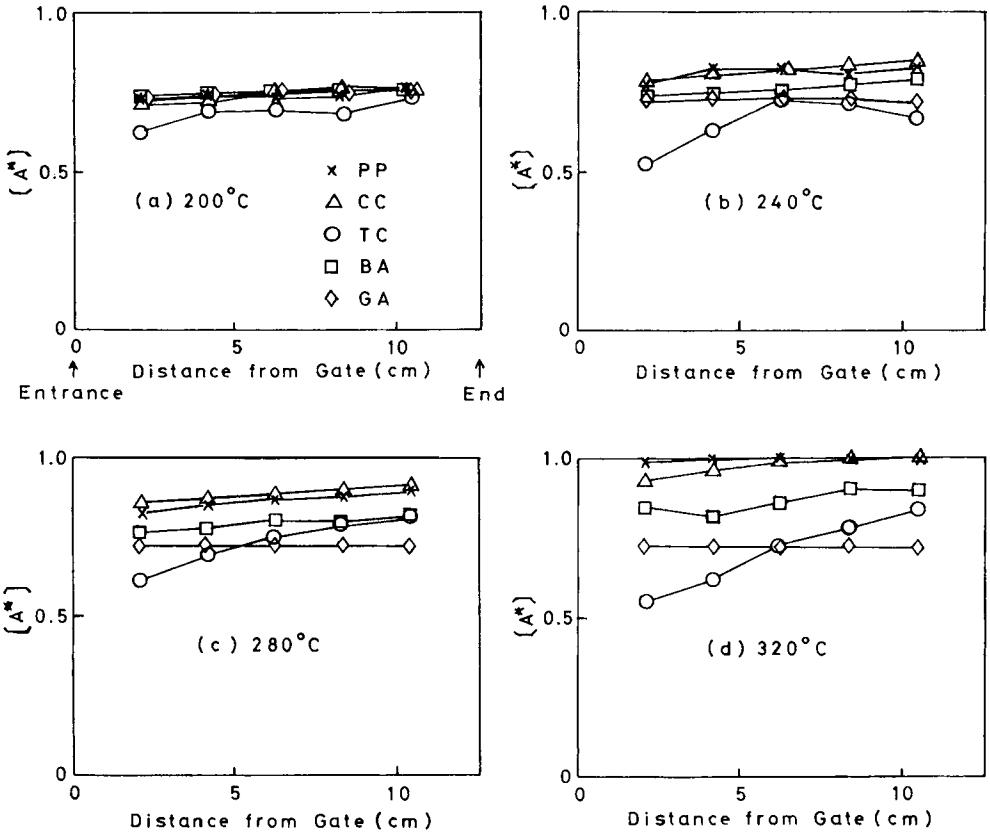

Figure 2 Distributions of a^*-axis-oriented component fraction $[A^*]$ in flow direction. Comparisons among samples. Cylinder temperature: (a) 200°C; (b) 240°C; (c) 280°C; (d) 320°C.

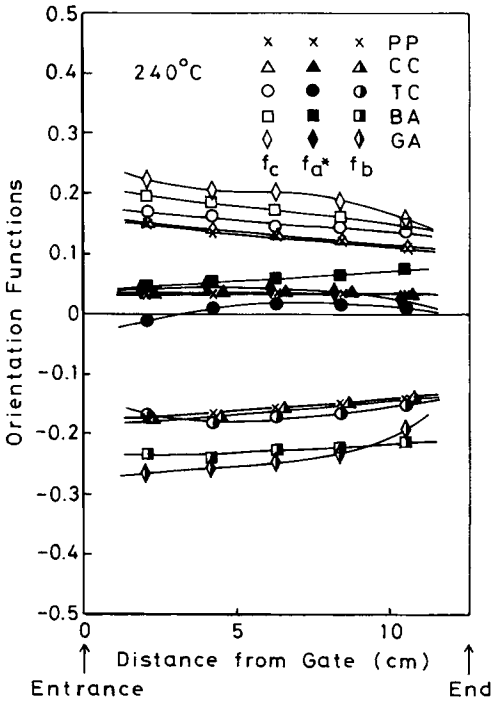

Figure 3 Distributions of orientation functions in flow direction. Cylinder temperature 240°C.

imens, it scarcely changes in the flow direction for the PP, CC, and GA specimens.

Figures 4(a)–(e) show the distributions of the c-axis orientation function f_c in the flow direction. As a large tendency, f_c is higher as the cylinder temperature is lower and decreases on going away from the gate. The dependence of f_c's of the BA and GA specimens on cylinder temperature is considerably weaker than that of the PP, CC, and TC specimens.

Figures 5(a)–(d) show comparisons of the distribution of f_c in the flow direction among samples. The order of f_c is GA > BA > TC > CC > PP and agrees with that of crystallization temperature.

Distribution of Higher-Order Structures in Thickness Direction

Figures 6(a)–(d) show the distributions of crystallinity X_c in the thickness direction. Here, H is a half of the thickness of specimen and y is the distance from the center. X_c is low at the surface region and increases toward the interior. This is because the inner region is cooled more slowly. Although not so much difference is observed among samples, it seems

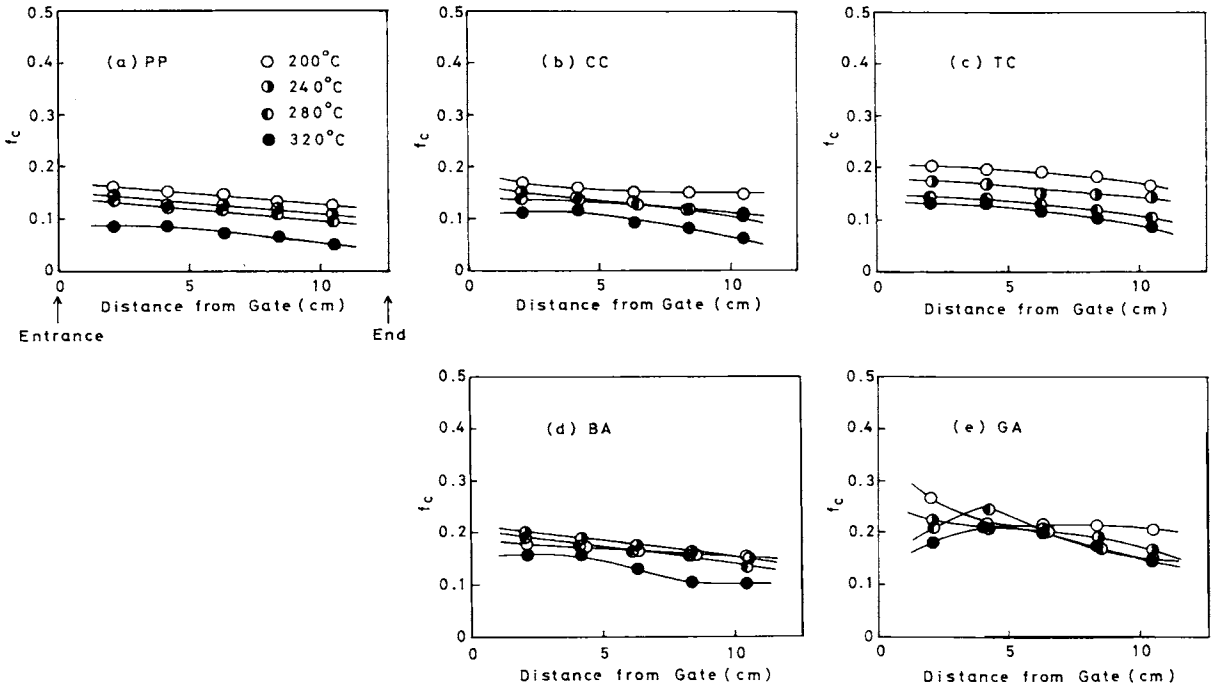

Figure 4 Distributions of c-axis orientation function f_c in flow direction. Influence of cylinder temperature: (a) PP; (b) CC; (c) TC; (d) BA; (e) GA.

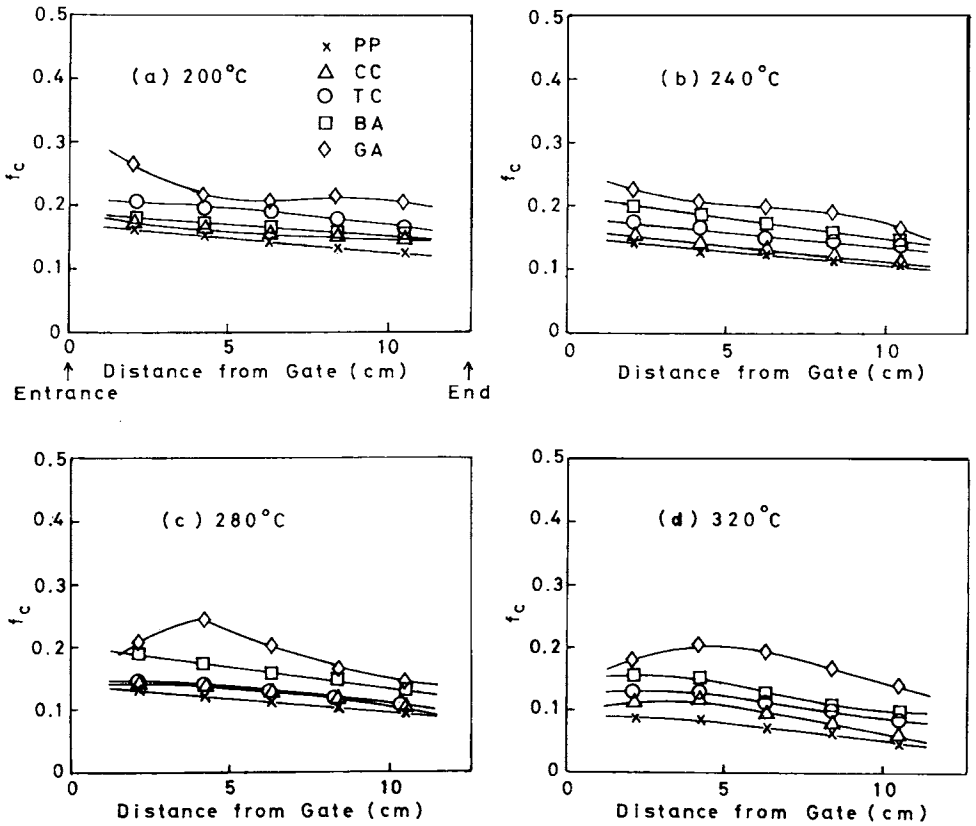

Figure 5 Distributions of c-axis orientation function f_c in flow direction. Comparisons among samples. Cylinder temperature; (a) 200°C; (b) 240°C; (c) 280°C; (d) 320°C.

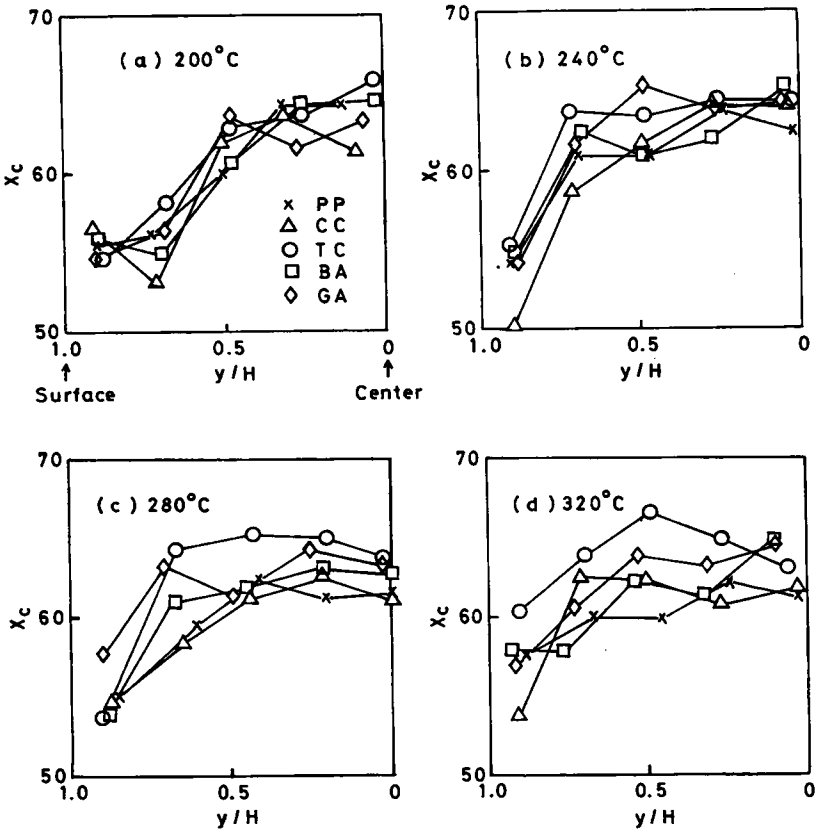

Figure 6 Distributions of crystallinity X_c in thickness direction. Comparisons among samples. Cylinder temperature: (a) 200°C; (b) 240°C; (c) 280°C; (d) 320°C.

that the TC and GA specimens show slightly higher X_c. It seems that cylinder temperature scarcely influences X_c.

Figures 7(a)–(e) show the distributions of β-crystal content, K value, in the thickness direction. Except for the surface region of the specimen molded from CC at a cylinder temperature of 200°C, the K value is higher nearer the surface and decreases toward the interior and is zero at the central region. The K value is higher as the cylinder temperature is lower. Although the addition of CC increases the K value, the addition of TC, BA, or GA, in particular, of GA, decreases it.

Figures 8(a)–(d) show the distributions in the thickness direction, of the wide-angle X-ray diffraction intensity ratio $I(040)/I(110)$, which expresses the degree of b-axis orientation to the thickness direction.[27] The lower the ratio, the higher the degree of b-axis orientation to the thickness direction. The PP and CC specimens show similar tendencies where the ratio is somewhat higher near the surface, decreases once, and increases toward the interior. The addition of CC scarcely influences the ratio. The TC specimens show very low ratios and long minimum regions. The BA specimens show maxima and the GA specimens show minima at midway regions. The crystal orientation state in injection moldings of talc-filled polypropylenes has been reported in detail in a previous paper.[27]

Figures 9(a)–(d) show the distributions of the a^*-axis-oriented component fraction $[A^*]$ in the thickness direction. In these figures, since the degree of molecular orientation is very low at around the central region, there is some problem in evaluating $[A^*]$ and the precision of $[A^*]$ is not good at around the central region. $[A^*]$ is generally low at the surface region and increases toward the interior. $[A^*]$'s at the surface regions of the PP and CC specimens are higher as the cylinder temperature is higher. The addition of CC scarcely changes $[A^*]$ and the addition of TC, BA, or GA considerably decreases $[A^*]$. Namely, the addition of nucleators increases the c-axis-oriented component as against to the a^*-axis-oriented component throughout whole range in the thickness direction.

Figure 10 exemplifies the distributions in the thickness direction, of crystalline orientation functions of each sample molded at a cylinder temperature of 240°C. Except for the GA specimens, the absolute values of f_c and f_b are higher nearer the

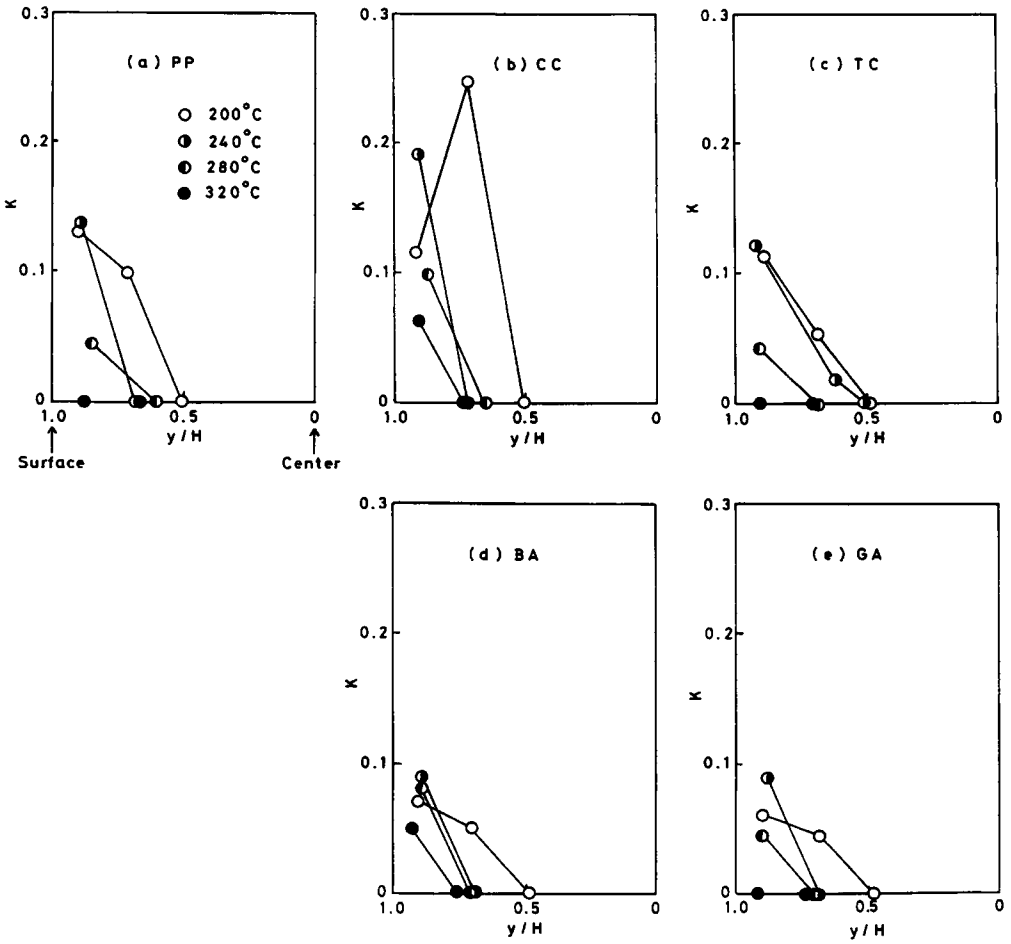

Figure 7 Distributions of β-crystal content, K value, in thickness direction. Influence of cylinder temperature: (a) PP; (b) CC; (c) TC; (d) BA; (e) GA.

surface and f_a· shows one or two maxima at midway regions. Similar results were obtained on the specimens molded at other cylinder temperatures.

Figures 11(a)–(e) show the distributions of the c-axis orientation function f_c in the thickness direction. Except for the GA specimens, f_c is higher nearer the surface and decreases toward the interior. f_c is higher as the cylinder temperature is lower at around the surface region. There are cases where a peak or a shoulder is observed at a midway position in the thickness direction at high cylinder temperatures.

Figures 12(a)–(d) show comparisons of the distribution of f_c in the thickness direction among samples. As a large tendency, f_c is increased by the addition of nucleators throughout whole range in the thickness direction.

DISCUSSION

We shall discuss on the distributions of two higher-order structures: crystallinity X_c and crystalline orientation f_c.

Figures 6(a)–(d) show that crystallinity X_c is low at the surface region and increases toward the interior. This is because the inner region is cooled more slowly. Houska and Brummell[19,20] measured X_c of an injection-molded polypropylene square plate from infrared spectrum and density and found that X_c showed a minimum at the surface skin region and increased toward the interior. Trotignon and Verdu[13,14] obtained X_c's of injection-molded polypropylenes from the heat of fusion measured by differential scanning calorimetry, which showed, contrary to the Houska et al. results, maxima at the skin regions, decreased once, and increased toward the interior. Since our, the Houska et al., and the Trotignon et al. results differ in the measuring method of X_c, they cannot be absolutely compared, particularly at the surface region of specimen where the degree of molecular orientation is high. However, they agree in the point that X_c increases toward the interior in the inner region where the degree of molecular orientation is low.

The distributions of crystalline orientation func-

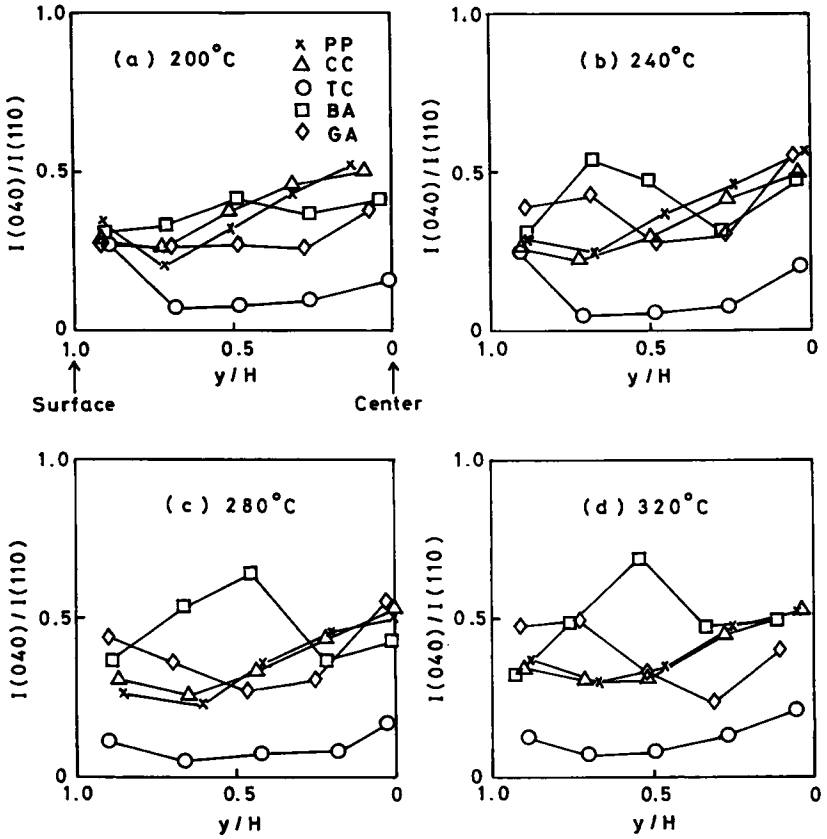

Figure 8 Distributions of wide-angle X-ray diffraction intensity ratio $I(040)/I(110)$ in thickness direction. Comparisons among samples. Cylinder temperature: (a) 200°C; (b) 240°C; (c) 280°C; (d) 320°C.

tions have been studied on injection moldings of high density polyethylenes by Kamal and Moy[33-35] and of polypropylenes[28] and talc- or calcium carbonate-filled polypropylenes[29] by the authors.

Figures 4 and 5 show that the crystalline c-axis orientation function f_c is higher as the cylinder temperature is lower and crystallization temperature T_c is higher and decreases on going away from the gate. The authors[28,29,36-38] have proposed a theoretical analysis of the molecular orientation process in injection molding based on a viewpoint of growth of a recoverable shear strain at the gate and its relaxation in the cavity. According to the authors' theory, the fact that f_c is higher as the cylinder temperature is lower is because the lower the cylinder temperature, the lower the injected resin temperature, which causes a higher melt orientation (recoverable shear strain) and a longer relaxation time of the recoverable shear strain. The fact that f_c is higher as T_c is higher is because the higher the crystallization temperature, the sooner the solidification and the less the relaxation of melt orientation (recoverable shear strain).

Trotignon et al.[8,13,14] measured on injection-molded polypropylenes the distributions in the flow direction of the crystalline orientation A, which was obtained from the (110) and (111) plane reflection intensities in wide-angle X-ray diffraction and of the crystalline and amorphous orientations, f_{cr} and f_{am}, by infrared dichroism, and found that these degrees of orientation decreased on going away from the gate. Murphy et al.[21,22] also obtained similar results on A for injection-molded polypropylenes. Altendorfer and Seitl[10] and Menges et al.[17,24] obtained similar results on the orientation degree measured by birefringence for injection-molded polypropylenes. Kubota[18] reported that the orientation degree measured by fluorescence showed a maximum at a midway part in the flow direction of a rectangular plate injection-molded from a polypropylene. Kamal et al.[12] measured, by infrared dichroism, the degrees of crystalline and amorphous orientations of an injection molding of polypropylene filled with 10 wt % glass fibers and found that both the orientations were increased by glass fiber filling and decreased on going away from the gate. The authors obtained

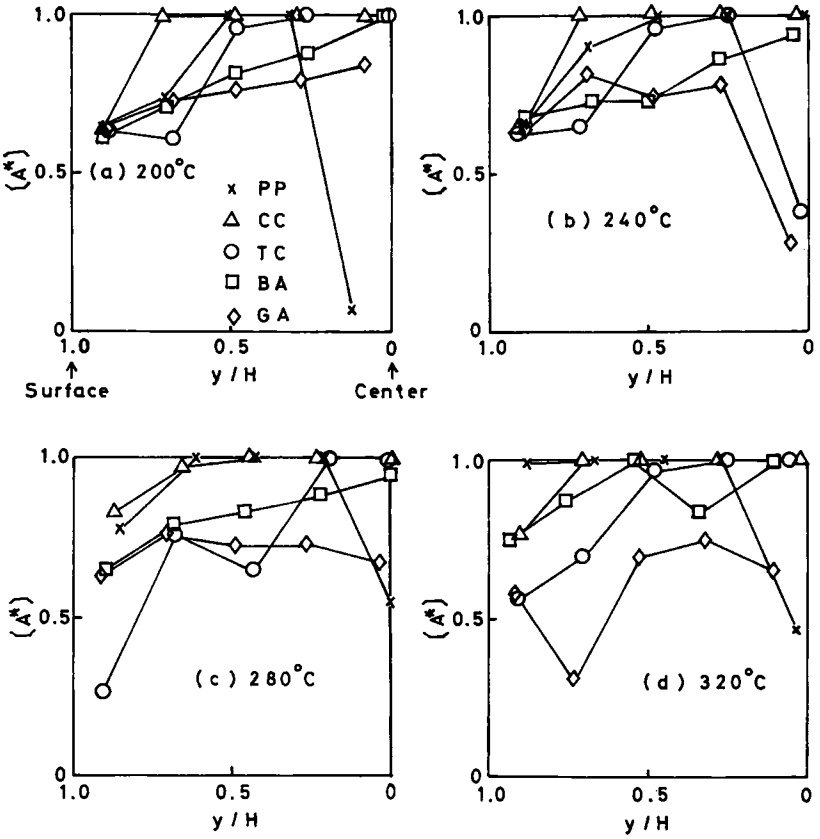

Figure 9 Distributions of a^*-axis-oriented component fraction $[A^*]$ in thickness direction. Comparisons among samples. Cylinder temperature: (a) 200°C; (b) 240°C; (c) 280°C; (d) 320°C.

similar results for injection moldings of polypropylenes[28] and talc- or calcium carbonate-filled polypropylenes.[29] Since a similar tendency was obtained also for injection moldings of nucleator-added polypropylenes in the present study, the fact that the degree of molecular orientation decreases on going away from the gate is considered general in injection moldings of thermoplastics. According to the authors' theory,[28,29,36–38] the fact that the degree of molecular orientation of an injection molding decreases on going away from the gate is because the flowing time of a molten resin increases on going away from the gate, which causes much relaxation of melt orientation (recoverable shear strain, in other word, degree of chain extension) during flow in the cavity.

Figures 11(a)–(e) show that f_c is higher nearer the surface and decreases toward the interior and that f_c is higher as the cylinder temperature is lower at around the surface region. According to the authors' theory,[28,29,36–38] the facts that f_c is higher nearer the surface and as the cylinder temperature is lower are because the lower the cylinder temperature, the lower the injected resin temperature, which causes a higher melt orientation (recoverable shear strain) and a longer relaxation time of the recoverable shear strain, and because the relaxation of the recoverable shear strain is less nearer the surface since the molten resin solidifies sooner nearer the surface.

There are cases where a peak or a shoulder is observed at a midway position in the thickness direction at high cylinder temperatures. This phenomenon is assumed to be caused by the secondary flow during the cooling and pressure holding process: When injection molding is carried out under a high holding pressure, the molten resin in the cavity solidifies progressively from the surface to the interior and the volume of the resin is reduced; an excess molten resin flows into the still molten inner region by the amount of the volume reduction by the action of holding pressure; this secondary flow is finished at the time of gate sealing; the higher the cylinder temperature, the higher the injected resin temperature, which takes a longer gate sealing time and causes a more secondary flow. Since, although the secondary flow is slow, it is a flow at a low temper-

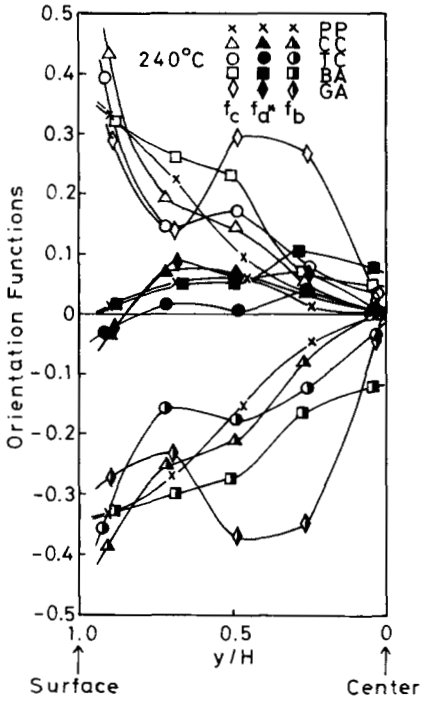

Figure 10 Distributions of crystalline orientation functions in thickness direction. Cylinder temperature; 240°C.

ature just before the solidification, it causes a high recoverable shear strain for slow flow, the relaxation time of the recoverable shear strain is long, and the time until solidification is short. Therefore, it is considered that, regardless of even a slight flow, it causes a notable molecular orientation. Particularly in the case of GA, since gelation occurs at temperatures below around 190°C, as shown in Figure 13, even a slight secondary flow may cause a high recoverable shear strain and the relaxation time of the recoverable shear strain is long, which is assumed to cause a notable molecular orientation.

Koppelmann et al.[15,16,23] measured the distributions in the thickness direction, of birefringences of injection-molded polypropylenes, and found that birefringences at the inner regions of specimens molded with holding pressures were higher than that molded without holding pressure. Hirose et al.,[7] Koppelmann et al.,[15,16,23] and Menges et al.[17] measured the distributions in the thickness direction, of birefringences of injection-molded polypropylenes, Trotignon and Verdu[13,14] measured the distributions in the thickness direction, of orientation degrees A of injection-molded polypropylenes by X-ray diffraction, and Trotignon and Verdu[13] and Houska

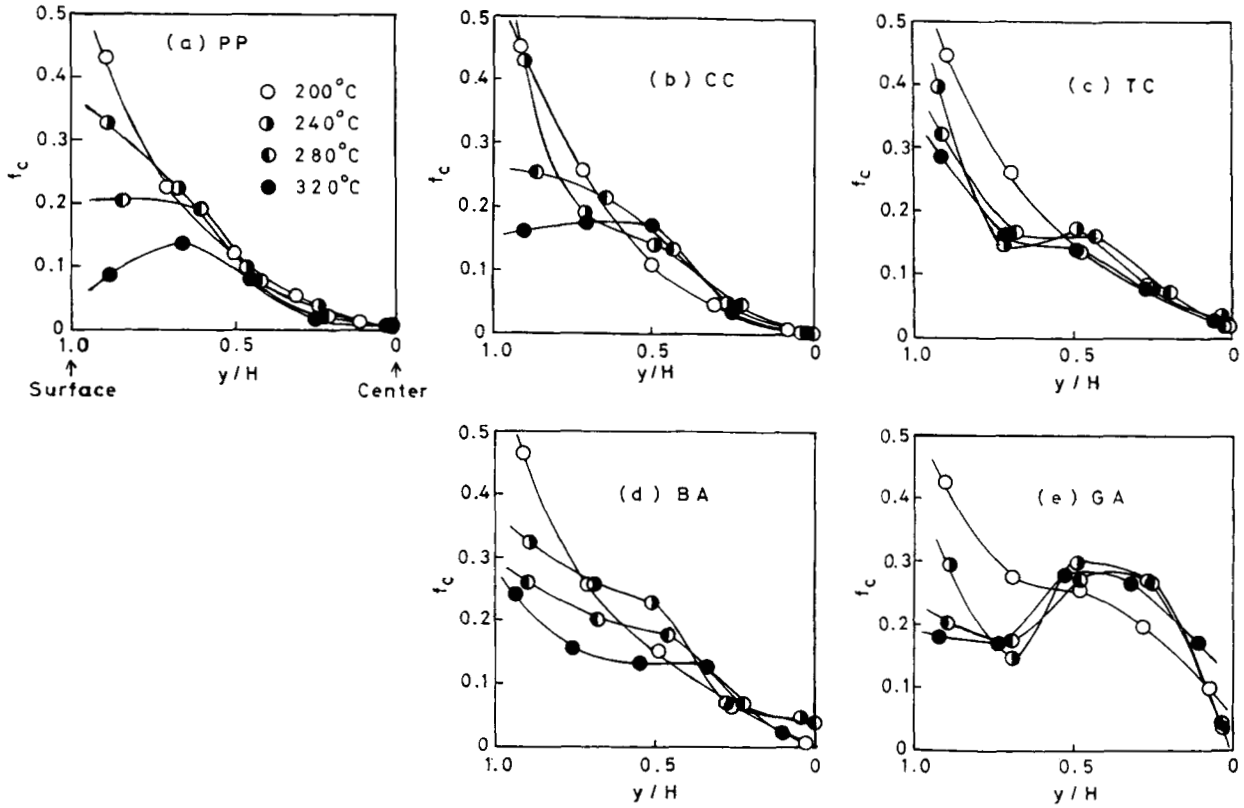

Figure 11 Distributions of c-axis orientation function f_c in thickness direction. Influence of cylinder temperature: (a) PP; (b) CC; (c) TC; (d) BA; (e) GA.

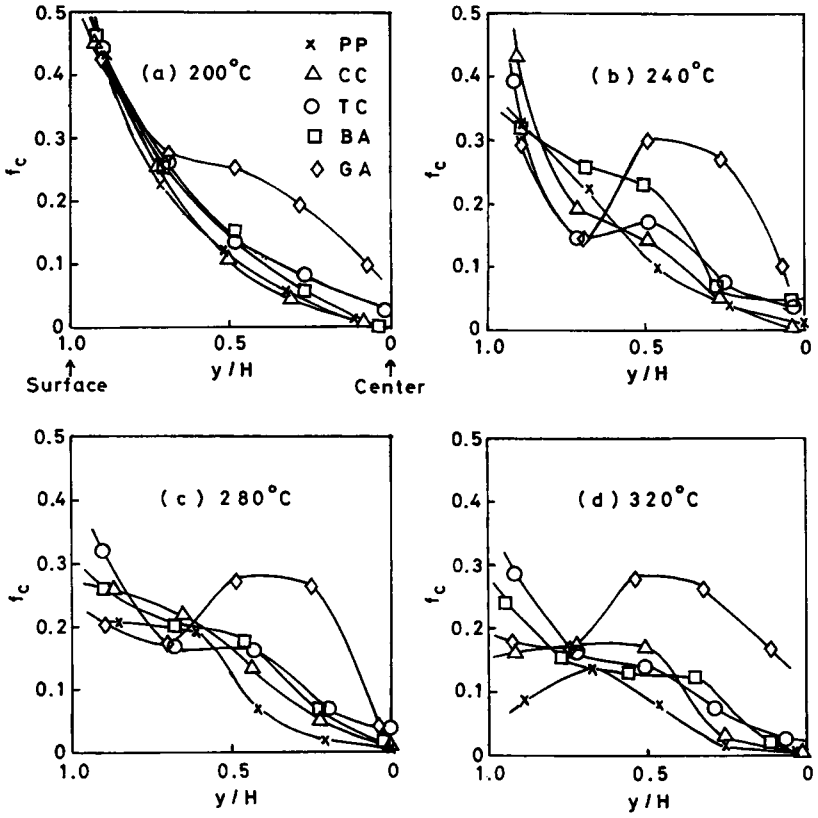

Figure 12 Distributions of c-axis orientation function f_c in thickness direction. Comparisons among samples. Cylinder temperature: (a) 200°C; (b) 240°C; (c) 280°C; (d) 320°C.

and Brummell[19,20] measured the distributions in the thickness direction, of crystalline and amorphous orientation functions, f_{cr} and f_{am}, of injection-molded polypropylenes by infrared dichroism. They all observed a maximum of molecular orientation at around the surface region. In the present experiment, however, as a possible reason, due to a large slicing interval, no such maximum was observed and f_c decreased gradually from the surface to the interior. Kubota[18] measured the distribution of the degree of fluorescent orientation of an injection-molded polypropylene in the thickness direction and found that no orientation maximum was observed at around the surface region and the degree of orientation decreased gradually from the surface to the interior as in the present results. Kamal et al.[12] measured on an injection molding of polypropylene filled with 10 wt % glass fibers the distributions in the thickness direction, of the degrees of crystalline and amorphous orientations by infrared dichroism and found that both the orientations were higher nearer the surface and were increased by the filling of glass fibers, agreeing with the present results. The authors measured on injection moldings of polypropylenes[28] and talc- or calcium carbonate-filled polypropylenes[29] the distributions of f_c in the thickness direction and obtained similar results to the present ones.

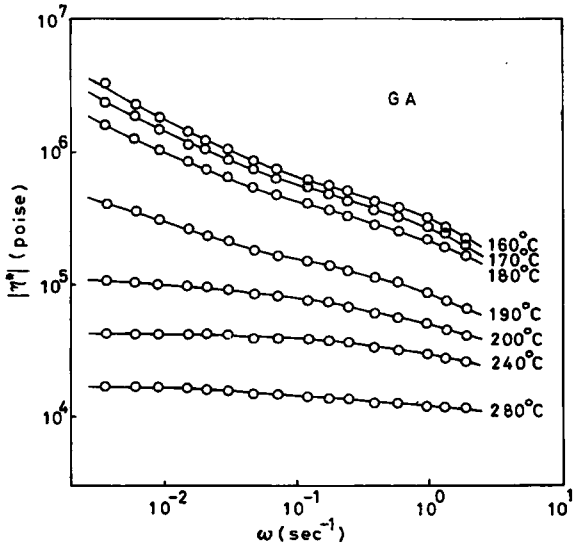

Figure 13 Temperature change of absolute value of complex viscosity $|\eta^*(\omega)|$ of GA sample.

Figures 12(a)–(d) show that f_c is increased by the addition of nucleators throughout the whole range in the thickness direction. This reason is why, since the samples with nucleators solidify faster than that without nucleator during the primary and secondary flows due to higher crystallization temperatures and hence due to lower supercoolings, $\Delta T = T_m - T_c$, less relaxation of the recoverable shear strain occurs.

CONCLUSIONS

Flexural test specimens were injection-molded from polypropylenes containing 0.5 wt % of calcium carbonate (CC), talc (TC), *p-tert*-dibutyl-benzoic acid monohydroxy aluminum (BA), or Gelall MD (GA) under cylinder temperatures of 200–320°C and distributions of higher-order structures in the flow and thickness directions were studied. The following results were obtained:

1. Distributions of higher-order structures in the flow direction:
   (i) The a^*-axis-oriented component fraction $[A^*]$ is higher as the cylinder temperature is higher and increases on going away from the gate. The TC specimens show high degrees of the increase. $[A^*]$ of the GA specimens scarcely changes with cylinder temperature and is uniform across the flow direction.
   (ii) The crystalline c-axis orientation function f_c is higher as the cylinder temperature is lower and decreases on going away from the gate. f_c is higher as the crystallization temperature is higher.
2. Distributions of higher-order structures in the thickness direction:
   (i) The crystallinity X_c is low at the surface region and increases toward the interior. The TC and GA specimens show slightly higher X_c than the other specimens.
   (ii) The β-crystals exist at the surface region and do not exist at the inner region. The β-crystal content is higher as the cylinder temperature is lower. Although the addition of CC increases the β-crystals, the addition of TC, BA, or GA decreases them.
   (iii) While the addition of TC greatly increases the b-axis orientation to the thickness direction, the addition of BA decreases it.
   (iv) $[A^*]$ is low at the surface region and increases toward the interior. Although the addition of CC scarcely changes $[A^*]$, the addition of TC, BA, or GA decreases it.
   (v) f_c is the highest at the surface region and decreases toward the interior. f_c at the surface region is higher as the cylinder temperature is lower. The addition of nucleators increases f_c. There are cases at high cylinder temperatures where the maximum of f_c is observed at a midway position in the thickness direction, which is assumed to be caused by the secondary flow during the cooling and pressure holding process. This phenomenon is particularly notable for the GA specimen which gelates at temperatures below around 190°C.
3. Study on molecular orientation process: A qualitative consideration was made on the molecular orientation process in injection molding from a viewpoint of growth of a recoverable shear strain at the gate and its relaxation in the cavity. It could explain all the above-mentioned experimental results concerning crystalline orientation f_c. For example, the fact that the addition of crystallization nucleators increases f_c is because it causes sooner solidification and the relaxation of melt orientation (recoverable shear strain) is less.

The authors would like to thank Tokuyama Soda Co., Ltd. for permission to publish this paper.

REFERENCES

1. M. R. Kantz, H. D. Newman, Jr., and F. H. Stigale, *J. Appl. Polym. Sci.*, **16**, 1249 (1972).
2. D. R. Fitchmun and Z. Mencik, *J. Polym. Sci. Polym. Phys. Ed.*, **11**, 951 (1973).
3. Z. Mencik and D. R. Fitchmun, *J. Polym. Sci. Polym. Phys. Ed.*, **11**, 973 (1973).
4. G. Menges, G. Wübken, and B. Horn, *Colloid Polym. Sci.*, **254**, 267 (1976).
5. A. Krsova, *Int. Polym. Sci. Technol.*, **4**(10), T/33 (1977).
6. K. Matsumoto, I. Miura, and K. Hayashida, *Kobunshi Ronbunshu*, **36**, 401 (1979).
7. H. Hirose, K. Ito, and T. Kawano, *Plastics Jpn.*, **26**(2), 13 (1980).
8. J. P. Trotignon, J. L. Lebrun, and J. Verdu, *Plast. Rubber Process. Appl.*, **2**, 247 (1982).

9. F. Altendorfer and G. Geymayer, *Plastverarbeiter,* **34,** 511 (1983).
10. F. Altendorfer and E. Seitl, *Plastverarbeiter,* **35,** 144 (1984).
11. F. Altendorfer and E. Seitl, *Kunststoffe,* **76,** 47 (1986).
12. M. R. Kamal, L. Song, and P. Singh, *SPE Tech. Pap., 44th ANTEC,* **32,** 133 (1986).
13. J. P. Trotignon and J. Verdu, *J. Appl. Polym. Sci.,* **34,** 1 (1987).
14. J. P. Trotignon and J. Verdu, *J. Appl. Polym. Sci.,* **34,** 19 (1987).
15. J. Koppelmann, E. Fleischmann, and G. Leiter, *Rheol. Acta,* **26,** 548 (1987).
16. E. Fleischmann and J. Koppelmann, *Kunststoffe,* **77,** 405 (1987).
17. G. Menges, H. Ries, and T. Wiegmann, *Kunststoffe,* **77,** 917 (1987).
18. S. Kubota, *Polym. Prepr. Jpn.,* **36,** 3677 (1987).
19. M. Houska and M. Brummell, *Polym. Eng. Sci.,* **27,** 917 (1987).
20. M. Houska and M. Brummell, *Plaste Kautschuk,* **35,** 83 (1988).
21. M. W. Murphy, K. Thomas, and M. J. Bevis, *Plast. Rubber Process. Appl.,* **9,** 3 (1988).
22. M. W. Murphy, K. Thomas, and M. J. Bevis, *Plast. Rubber Process. Appl.,* **9,** 117 (1988).
23. E. Fleischmann and J. Koppelmann, *Kunststoffe,* **78,** 453 (1988).
24. G. Menges, A. Troost, J. Koske, H. Ries, and H. Stabrey, *Kunststoffe,* **78,** 806 (1988).
25. E. Fleischmann, P. Zipper, A. Jánosi, W. Geymayer, J. Koppelmann, and J. Schurz, *Polym. Eng. Sci.,* **29,** 835 (1989).
26. E. Fleischmann, *Int. Polym. Process.,* **4,** 158 (1989).
27. M. Fujiyama and T. Wakino, *J. Appl. Polym. Sci.,* to appear.
28. M. Fujiyama and T. Wakino, *J. Appl. Polym. Sci.,* to appear.
29. M. Fujiyama and T. Wakino, *J. Appl. Polym. Sci.,* to appear.
30. M. Fujiyama and T. Wakino, *J. Appl. Polym. Sci.,* **42,** 2739 (1991).
31. W. Weidinger and P. H. Hermans, *Makromol. Chem.,* **50,** 98 (1961).
32. A. Turner-Jones, J. M. Aizilewood, and D. R. Beckert, *Makromol. Chem.,* **75,** 134 (1964).
33. F. H. Moy and M. R. Kamal, *Polym. Eng. Sci.,* **20,** 957 (1980).
34. M. R. Kamal and F. H. Moy, *Polym. Eng. Rev.,* **2,** 381 (1983).
35. M. R. Kamal and F. H. Moy, *J. Appl. Polym. Sci.,* **28,** 1787 (1983).
36. M. Fujiyama, *Nihon Reoroji Gakkaishi,* **14,** 152 (1986).
37. M. Fujiyama, Y. Kawasaki, and T. Wakino, *Nihon Reoroji Gakkaishi,* **15,** 191 (1987).
38. M. Fujiyama, Y. Kawasaki, and T. Wakino, *Nihon Reoroji Gakkaishi,* **15,** 203 (1987).

Received March 13, 1990
Accepted July 24, 1990